BURNING VELOCITY AND FLAME STRUCTURE OF METHANE FLAMES INHIBITED WITH HEPTAFLUOROPROPANE (C_3HF_7)

Caimao Luo, Bogdan Z. Dlugogorski and Eric M. Kennedy
Process Safety and Environment Protection Research Group
School of Engineering
The University of Newcastle
Callaghan, NSW 2308, AUSTRALIA
Email: Eric.Kennedy@newcastle.edu.au
Fax: +61 2 4921 6920

ABSTRACT

This paper updated the two existing flame inhibition mechanisms for C_3HF_7 (FM-200^{TM}) of Sanogo et al. and Williams et al. using the sensitivity analysis of the burning velocity as the criterion. GRI Mech 3.0 was deployed to model the combustion of methane. The results of the modified mechanisms were then compared with the published experimental measurements of (i) flame structure for $CH_4/O_2/Ar$ premixed flames inhibited by 1.0% C_3HF_7 as derived from the molecular beam-mass spectrometry (MBMS) data and (ii) low pressure (10 torr) stoichiometric CH_4/O_2 premixed flames inhibited by 4.0% C_3HF_7 as obtained from experiments involving the laser-induced fluorescence (LIF). The numerical calculations were performed with the aid of PREMIX computer code for burner stabilised (flame structure) and freely propagating (burning velocity) flames. The inlet boundary condition was modified to allow a direct specification of the inlet composition for all species. The results of the computation indicate that both modified mechanisms yield similar burning velocities and similar concentration profiles of major species. This means that, the simpler mechanism of Sanogo et al., as modified in the present work, can be used in scoping studies where a large number of cases need to be run rapidly or to obtain an interim solution for further optimisation with the modified mechanism of Williams et al.

INTRODUCTION

The Montreal Protocol necessitated the phase out of halons from production in industrialised countries by 1 January 1994. Among the potential replacements of halons, C_3HF_7 (HFC-227ea, or heptafluoropropane), C_2HF_5 (HFC-125) and CF_3I (halon 13001) were tested in engine nacelle by The National Institute of Standard and Technology in the USA (NIST) as described by Hamins and Cleary (1995). According to the review included in the US EPA SNAP list, only C_3HF_7 possesses an extinguishing concentration lower than its NOAEL (no observed adverse effect level), indicating that it can be used against fires in occupied species. Its design extinguishing concentration is 7% by volume, according to Harrison (1995). Another advantage of C_3HF_7 is its zero ozone depletion potential number (ODP). Finally, heptafluoropropane is a widely used agent in a number of applications, which adds a practical perspective to fundamental studies on its properties.

Modelling the inhibition mechanism of C_3HF_7 was conducted by Sanogo et al. (1997), Hynes et al. (1998) and Williams et al. (2000) using hydrogen and methane as fuels. Starting from Westbrook's HF inhibition mechanism, Sanogo et al. added and modified the rate constants of

a number of reactions. These researchers have constructed the comprehensive chemical mechanism by combining the modified C_3HF_7 sub-mechanism with the Warnatz-methane oxidation sub-mechanism. Sanogo et al. predicted mole fraction profiles of CO_2, O_2, H_2O, O, C_3HF_7, HF and CF_2CH_2, with the profiles corresponding reasonably well with their experimental results derived from molecular beam and mass spectroscopy (MBMS) measurements for mitigated premixed methane flames ($CH_4/Ar/O_2/C_3HF_7$ = 0.168/0.336/ 0.486/0.01), stabilised on water-cooled flat-burner, at 0.042 atm.

Hynes et al. (1998) employed a new comprehensive mechanism, comprising GRI-Mech 1.2 for hydrogen and light alkane combustion, the NIST hydrofluorocarbon mechanism (NIST HFC), and the C_3HF_7 mechanism developed by themselves to model the $\phi = 0.4$ hydrogen-air premixed flames inhibited by 1.0 and 3.2 % of C_3HF_7 by volume. Williams et al. (2000) made some modifications to Hynes' C_3F_7H mechanism to tune its performance to low-pressure conditions and modelled the stoichiometric methane-oxygen premixed flame inhibited by 4% of C_3HF_7 at low pressure of 10 torr ($CH_4/O_2/C_3HF_7$ = 0.32/0.64/0.04). Since Williams' mechanism originated from Hynes' mechanism, it could be denoted as the updated Hynes' mechanism. Williams et al. compared their predicted flame structure with the laser-induced fluorescence (LIF) measurements of H, OH, CH, CF_2, CHF and CF radicals. Their comparison was limited to the shape and peak locations of the predicted and measured flame structures, which agreed well for OH and CH radicals, because LIF measurements can only account for relative amplitudes of the concentration profiles. They also compared the predicted burning velocities under atmospheric conditions for lean CH_4/O_2 (ϕ = 0.45, 0.5 and 0.55) premixed flames inhibited by 2.96, 2.93 and 2.91% of C_3HF_7 to experimental measurements of Linteris et al. (2000), obtaining the relative errors of 17, 11, 30% respectively. Note that Sanogo's inhibition mechanism, which combined Westbrook's HF sub-mechanism and C_3HF_7 inhibition sub-mechanism, includes a smaller number of species and elementary reactions. It is a shorter mechanism requiring less computational resources and allowing faster convergence than Williams' mechanism.

In this article, we will update Williams' C_3HF_7 mechanism and Sanogo's C_3HF_7 inhibition mechanisms based on the sensitivity analysis of the burning velocity. We will then investigate the performance of both mechanisms in predicting the flame structure, and compare the results with the available experimental measurements.

NUMERICAL MODELLING

GRI Mech 3.0 was adopted in this study, with all reactions involving nitrogen deleted from the mechanism. The NIST HFC mechanism was employed to characterise hydrofluorocarbon oxidation chemistry. In this HFC mechanism, we updated some reaction rate coefficients according to L'Esperance et al. (1999) and Linteris and Truett (1996). To study the effect of different comprehensive mechanisms on the burning velocity and flame structure, five combinations of comprehensive mechanisms, as listed in Table 1, were employed in the computations. The transport and thermodynamic properties of species appearing in C_3HF_7 mechanisms were obtained from Professor Mackie (2003) by private communication and applied to all simulations. In conjunction with the mechanistic choices listed in Table 1, this has important implications. For example, the original mechanism of Sanogo et al. (1997) varies from the mechanism numbered 2 in Table 1 owing to the different sources of the thermodynamic and transport data bases, and the different methane oxidation mechanism.

Table 1: The reaction mechanisms employed in the present study.

Mech.	Sub-mechanisms	Reference	Species	Reactions
1	GRI-Mech 3.0 + NIST HFC + updated Williams' C_3HF_7 mechanism	Present work	99	856
2	GRI-Mech 3.0 + Sanogo C_3HF_7 mechanism	Sanogo et al. (1997)	55	273
3	GRI-Mech 3.0 + NIST HFC + Williams' C_3HF_7 mechanism	Williams et al. (2000)	99	856
4	Hynes C_3HF_7 mechanism	Hynes et al. (1998)	92	807
5	GRI-Mech 3.0 + updated Sanogo's C_3HF_7 mechanism	Present work	55	273

The commercially available PREMIX computer program, developed at Sandia National Laboratories, was employed to perform both the kinetic calculation and the sensitivity analysis (Kee et al., 1989). To save the CPU time, the calculations were performed for mixture-based transport properties and with no Soret diffusion. The effects of Soret diffusion and the multi-component thermal diffusion coefficients were examined. Their inclusion in the calculations was found to lead to insignificant differences in the results.

In several cases, to obtain a convergence, the parameter defining the frequency of calculating the Jacobian matrix (NJAC) was increased gradually from 5 to 40, to mean that the Jacobian matrix in Newtonian iteration was updated every NJAC (5 to 40) times. The effects of varying NJAC and TJAC were studied by varying NJAC from 40 to 5 and TJAC from 40 to 10, resulting in virtually unaltered solutions. Varying the absolute and relative tolerances on the Newtonian iterations and on the time steps (ATOL, RTOL, ATIM and RTIM) showed that while these parameters can affect the convergence, depending on the input (including the input kinetic mechanism), they had little influence on the resulting number of grid points. Furthermore, once a convergent solution was obtained, the continuation keyword (CNTN) was extensively employed to progress the solution to new conditions.

The choices of values for GRAD and CURV keywords define the number of grid points that ultimately determine the accuracy of the computed laminar burning velocity. The laminar burning velocity tends to decrease proportionally to the reciprocal of the number of grid points Dlugogorski et al. (1998). In the current work, we set CURV and GRAD to 0.5 and 0.2, respectively. The effect of selecting relatively large values of these parameters, which were necessary owing to the CPU considerations, was factored out by reporting the laminar burning velocities of mitigated flames normalised with laminar burning velocity of non-mitigated stoichiometric flames.

The calculations were performed for freely propagating flames (keyword FREE), to obtain valued of the burning velocity, and burner stabilised flames (keyword BURN), to obtain the flame structure. The calculations of the burning velocity included the solution of the energy equation to obtain a temperature profile, whereas for the calculations of the flame structure the temperature profile, as measured in experiments, was used instead. In the latter case, this approach simplified the complexity of the calculations and resulted in a shorter calculation time.

For all the computational cases in this study, we explicitly specified the mass fractions at the inlets for all species, or $y_{k,1} = \varepsilon_{k,1}$, instead of

$$y_{k,1} = \varepsilon_{k,1} - \left(\frac{\rho A y_k V_k}{\dot{m}} \right)_{j=1\frac{1}{2}}$$

as done in the PREMIX code; where $y_{k,1}$ is the mass fraction of species k at node 1, $\varepsilon_{k,1}$ the inlet reactant fraction of the kth species, V_k the diffusion velocity of kth species, ρ the mixture density, $\dot{m}$ the mass flowing rate. The boundary condition used by PREMIX changes the imposed composition of the inlet mixture. The effect of the selection of the boundary condition becomes more amplified for steep temperature gradients at the inlet, which occurs frequently for burner-stabilised flames. To illustrate this consideration, we compare the flame structure of $CH_4/O_2/Ar/C_3HF_7$ premixed flames with the measurements of Sanogo et al. (1997), including their temperature profiles illustrated in Figure 1 with the original measurements provided by Professor Vovelle (2003) by private communication.

The two temperature profiles correspond to thermocouples placed 0.2 and 20 mm from the skimmer's cone of the mass beam apparatus. It is readily seen that because of its intrusive nature, the skimmer significantly modified the local temperature field adding to the uncertainty of the concentration measurements. For this reason, both temperature profiles were used in the calculations to gauge the effect of heat transfer to the skimmer on the flame structure reported by Sanogo et al. The modification of this boundary condition affects the concentration profiles of concentrations of the major species, as shown in Figure 2. However, the modification of the inlet boundary condition has less pronounced effect on the concentration of the intermediate species, as illustrated in Figure 3.

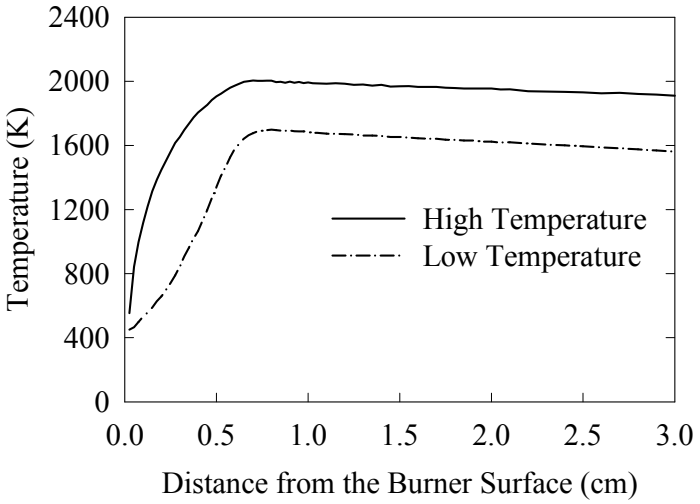

Figure 1: Temperature profiles used as the inputs to modelling of premixed methane burner stabilised $CH_4/O_2/Ar/1\%\ C_3HF_7$ premixed flames.

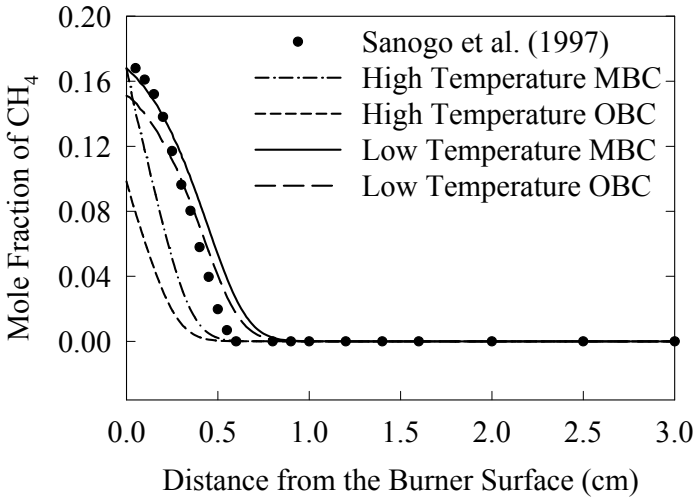

Figure 2: Comparisons of CH_4 species predictions using PREMIX-provided (called original-BC, or OBC) and modified-BC (or MBC) with experimental measurements by Sanogo et al. (1997).

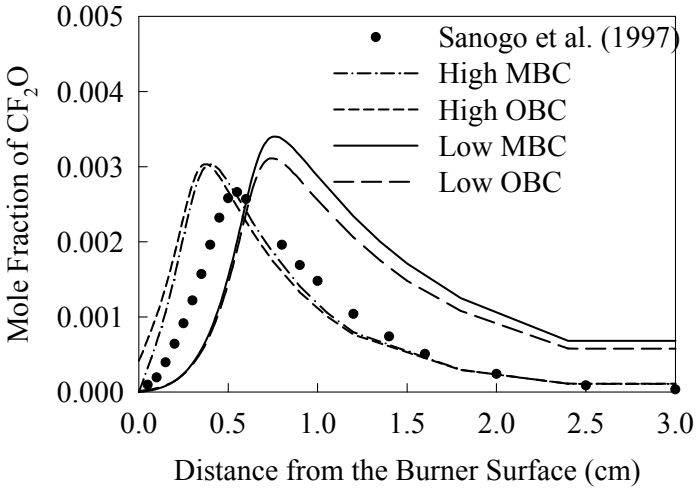

Figure 3: Comparisons of CF_2O species predictions using PREMIX-provided (called original-BC) and modified-boundary conditions with experimental measurements by Sanogo et al. (1997).

RESULTS AND DISCUSSION

Mechanism of Sanogo et al.

Sanogo's mechanism (published in 1997) contains substantially fewer species and elementary reactions than Williams' mechanism (published in 2000). Nonetheless, Sanogo's mechanism has been proven successful in simulating the concentration of the major species in flames, at a fraction of the computational effort necessary for Williams' mechanism. Hence, it is

worthwhile to update this mechanism for the benefit of future researchers who may wish to obtain rapidly converged solutions.

Based on the sensitivity analysis of the burning velocity, as shown in Figure 4, for the GRI-Mech 3.0 in conjunction with Sanogo's C_3HF_7 inhibition mechanism, we updated some rate coefficients and itemised them in Table 2. Because the original Sanogo's mechanism under-predicted the burning velocity, only the reactions with positive sensitivity coefficients were updated. For reactions R1 and R2, the pre-exponential factors were increased from the original 1.5×10^{11} and 1.4×10^{14} to 4.2×10^{12} and 2.8×10^{14} respectively. For R2, Knyazev et al. (1997) estimated the pre-exponential factor as 1.1×10^{15} for the temperature range from 951 to 1050 K. Therefore, even when doubled, the adjusted pre-exponential factor for R2 is still below the estimation of Knyazev et al. For reactions with the negative sensitivity coefficients, such as reactions R3 and R4, the pre-exponential factors were decreased from the original 2.0×10^{14} and 1.5×10^{13} to 2.5×10^{13} and 7.5×10^{12} respectively. The rate coefficient for R3 is from Richter et al. (1994). Rate coefficients for R1 and R4 are estimated by tuning the burning velocity.

$CH_2CF_2 + O \rightarrow CF_2O + CH_2$	R1
$CFO + M \rightarrow CO + F + M$	R2
$CFO + H \rightarrow CO + HF$	R3
$CH_2CF_2 + O \rightarrow CH_2O + CF_2$	R4

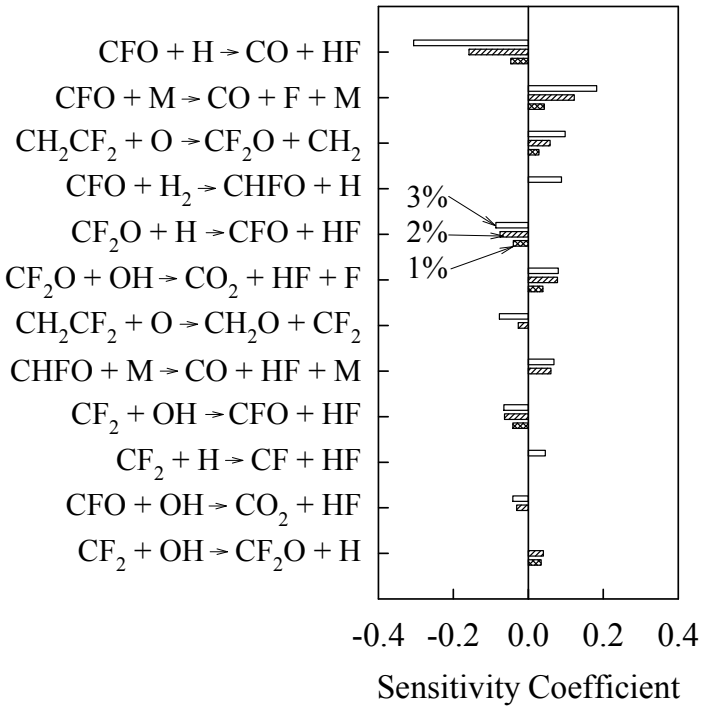

Figure 4: Sensitivity analysis of the laminar burning velocity for Sanogo's original C_3HF_7 inhibition mechanism for 1-3% C_3HF_7 added to stoichiometric methane-air premixed flames. The sensitivity coefficients were normalised with the sensitivity

coefficient of 0.30, 0.28 and 0.40 for $H + O_2 \rightarrow O + OH$ corresponding to 1, 2, and 3% of C_3HF_7.

Table 2: Modifications to Sanogo's mechanism (in units of cm, mole, cal, K, and s).

Reactions	A (original)	n (orig.)	E_a (original)	A (modified)	n (modif.)	E_a (modif.)	Reference
$CF_3+H\rightarrow CF_2+HF$	5.5E+13	0	0	5.3E+13	0	0	Takahashi et al. (1998)
$CF_3+O\rightarrow CF_2O+F$	1.3E+14	0	2000	9.3E+36	0	0	Takahashi et al. (1998)
$CF_3+CH_3\rightarrow CH_2CF_2+HF$	6.8E+13	0	0	2.5E+13	0	0	
$CHF_3+H\rightarrow CF_3+H_2$	5.0E+12	0	5000	3.7E+13	0	14600	Hranisavlejvic et al. (1998)
$CF_3+H_2\rightarrow CHF_3+H$				1.5E+13	0	17000	Hranisavlejvic et al. (1998)
$CF_2+H\rightarrow CF+HF$	2.0E+13	0	0	4.0E+13	0	0	Yamamori et al. (1999)
$CF_2+OH\rightarrow CFO+HF$	1.0E+13	0	0	3.0E+13	0	0	Biordi et al. (1976)
$CH_2CF_2+OH\rightarrow CF_2O+CH_3$	1.0E+13	0	0	2.0E+13	0	0	Estimated
$CH_2CF_2+O\rightarrow CH_2O+CF_2$	1.5E+13	0	0	7.5E+12	0	0	Estimated
$CH_2CF_2+O\rightarrow CF_2O+CH_2$	1.5E+11	0	0	4.2E+12	0	2280	Cvetanovic (1987)
$CF_2O+H\rightarrow CFO+HF$	1.3E+11	0	0	3.6E+09	1	36000	Zachariah and Tsang (1995)
$CF_2O+OH\rightarrow CO_2+HF+F$	7.6E+11	0	0	1.5E+12	0	0	Increased 2 times
$CFO+M\rightarrow CO+F+M$	1.4E+14	0	30000	2.8E+14	0	30000	Increased 2 times
$CFO+OH\rightarrow CO_2+HF$	1.0E+14	0	0	5.0E+13	0	0	Decreased 2 times
$CFO+H\rightarrow CO+HF$	2.0E+14	0	0	2.5E+13	0	0	Richter et al. (1994)
$CF+OH\rightarrow CO+HF$	1.0E+13	0	0	5.0E+12	0	0	Decreased 2 times
$CHFO+H\rightarrow CFO+H_2$	1.1E+08	1.8	2990	6.5E+07	1.8	2990	Decreased 2 times

As shown in Figure 5, the predictions of the modified mechanism agree well with experimental data. Note that, the original mechanism under-predicts the experimental burning velocity, indicating the success of applying the results of the sensitivity analysis to update the critical rate coefficients in order to improve the comparison with experiments. It should be stressed again that the Sanogo's mechanism as invoked in this study is different from that in Sanogo et al. (1997), for the reason explained in the first paragraph of the section on numerical modelling.

Mechanism of Williams et al.

According to the results of the sensitivity analysis of the burning velocity as shown in Figure 6 for original Williams' mechanism, the most sensitive reaction among those involving fluorine is R2. The original rate coefficients for the reverse reaction of R2 in the NIST HFC mechanism were the estimated values by Burgess et al. (1995). For reaction R2 in the forward direction, we replaced the original coefficients calculated by CHEMKIN with the experimentally determined values of Knyazev et al. (1997). These experimental coefficients are valid for temperature range between 951 and 1050 K under low pressure. Rate coefficients of reaction R5, which has a significant impact on the burning velocity are updated with rate parameters proposed by Yamamori et al. (1999). The rate coefficients proposed by Tsai and McFadden (1989) are valid for temperature 298 K only, while those of Yamamori et al. are valid for the temperature range between 1450 and 1860 K under low pressure. The other two reactions R6 and R7 are also updated with the values of the rate coefficients quoted in Table 3. With these modifications, the updated NIST HFC mechanism provides much

improved prediction of the burning velocity. Figure 7 illustrates the comparison between the experimental data of Linteris et al. (1998) and the present results.

$CF_2 + H \rightarrow CF + HF$ R5
$CF_3 + H \rightarrow CF_2 + HF$ R6
$CHFO + M \rightarrow CO + HF + M$ R7

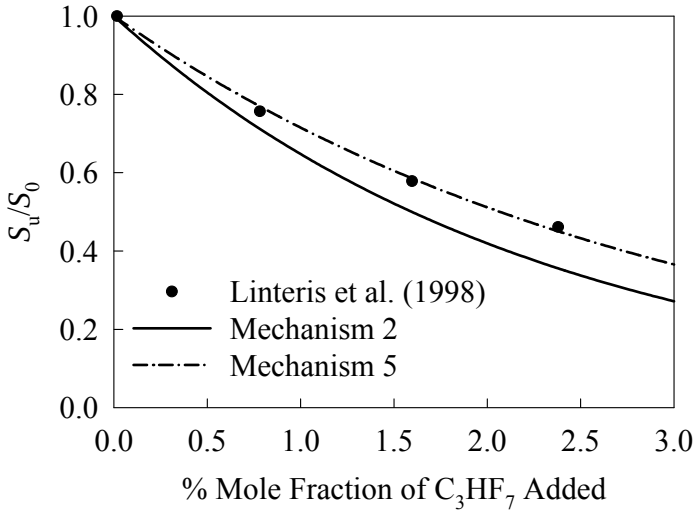

Figure 5: Comparison of burning velocity profiles as a function of concentrations of C_3HF_7 using the original and modified Sanogo's inhibition mechanisms with experimental data of Linteris et al. (1998).

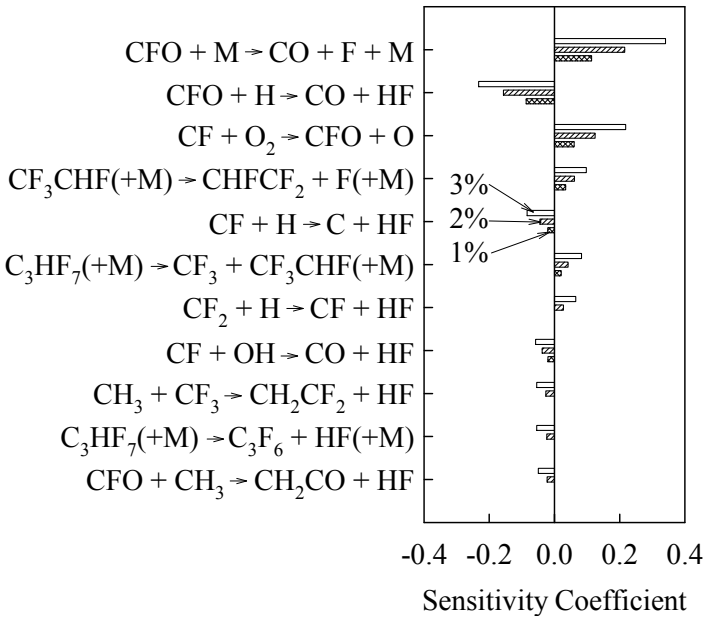

Figure 6: Sensitivity analysis of the laminar burning velocity for Williams' original C_3HF_7 inhibition mechanism for 1.0-3.0% C_3HF_7 added to stoichiometric methane-air premixed flames. The sensitivity coefficients were normalised with the sensitivity coefficient of 0.31, 0.24 and 0.21 for $H + O_2 \rightarrow O + OH$ corresponding to 1, 2, and 3% of C_3HF_7.

The choice of a kinetic mechanism depends on the purpose of a study. If the purpose is to account for all species, including all minor species and transitional species, one must select the modified Williams' mechanism as developed in this section, since this mechanism is more comprehensive. Thus our recommendation is to use modified Williams' mechanism first in an attempt to obtain a converged solution. If this is unsuccessful or the convergence procedure necessitates substantial computational time, one should attempt to employ the Sanogo's mechanism first.

Table 3: Modifications to NIST HFC inhibition mechanism (in units of cm, mole, cal, K, s)

Reactions	A (original)	n (orig.)	E_a (original)	A (modified)	n (modif.)	E_a (modified)	Reference
R2: CFO+M→CO+F+M	-	-	-	1.1e15	0.0	28200	Knyazev et al. (1997)
R2': CO+F+M→CFO+M	3.1e19	-1.4	-487	-	-	-	NIST estimate
R5: CF_2+H→CF+HF	2.0E+13	0	1250	4.0E+13	0	0	Yamamori et al. (1999)
R6: CF_3+H→CF_2+HF	5.5E+13	0	0	5.3E+13	0	0	Takahashi et al. (1998)
R7: CHFO+M→CO+HF+M	2.5E25	-3.0	43000	5.5e14	0.0	35200	Saito et al. (1985)

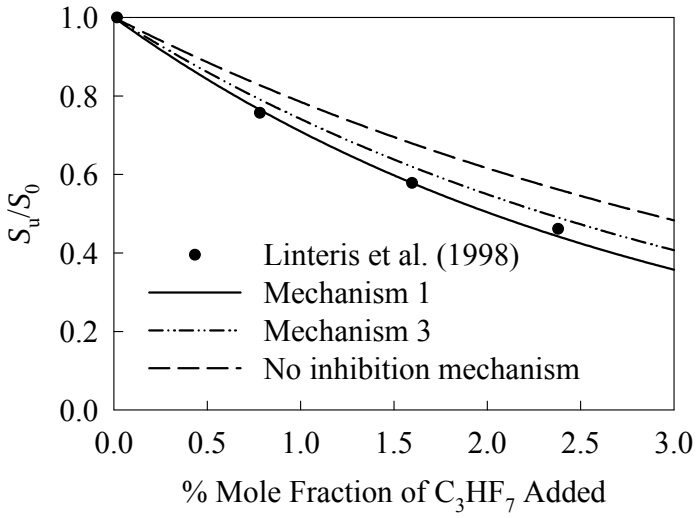

Figure 7: Comparison of the burning velocity, as a function of concentrations of C_3HF_7 among the modelled results of the original and modified Williams' inhibition mechanisms and experimental measurements of Linteris et al. (1998).

Flame Structure

There exist no significant differences in the concentration profiles of HF, C_3HF_7 and OH calculated from the various inhibition mechanisms. As illustrated in Figure 8, for distances lower than 0.6 cm, all mechanisms predict almost identical HF concentrations. For distances

higher than 0.6 cm, only Sanogo's mechanism predicts a slightly higher concentration of HF. Similar comments can be made for other species. As indicated in Figure 9, all mechanisms predict essentially the same consumption profiles of C_3HF_7, which agree with the experimental measurements. All mechanisms also yield similar profiles for OH, as illustrated in Figure 10, though they all under-predict the experimental measurement of the concentration of this radical. However, this lack of agreement may not necessarily point to problems with the rate coefficients of the reactions involving OH in the mechanisms, due to a good comparison of the predicted OH concentration with the experimental measurements of Williams et al. (2000) as shown in Figure 11.

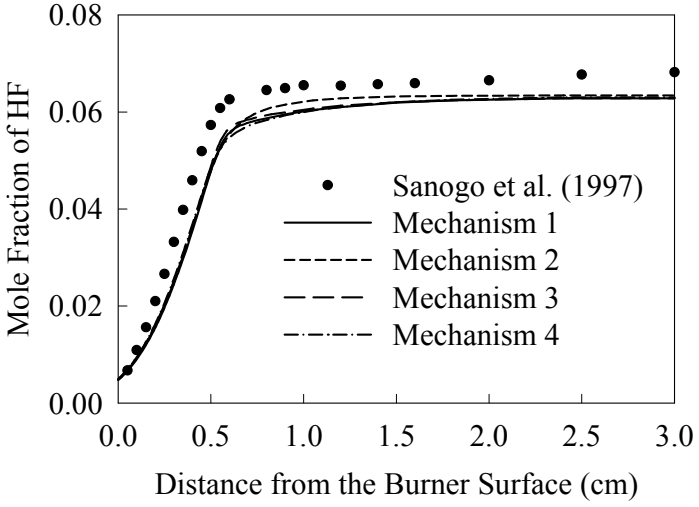

Figure 8: Comparison of the profiles of HF mole fraction produced by the mechanisms considered in this chapter with the experimental measurements of Sanogo et al. (1997); $CH_4/Ar/O_2/C_3HF_7 = 0.168/0.336/0.486/0.01$, $p = 0.042$ atm.

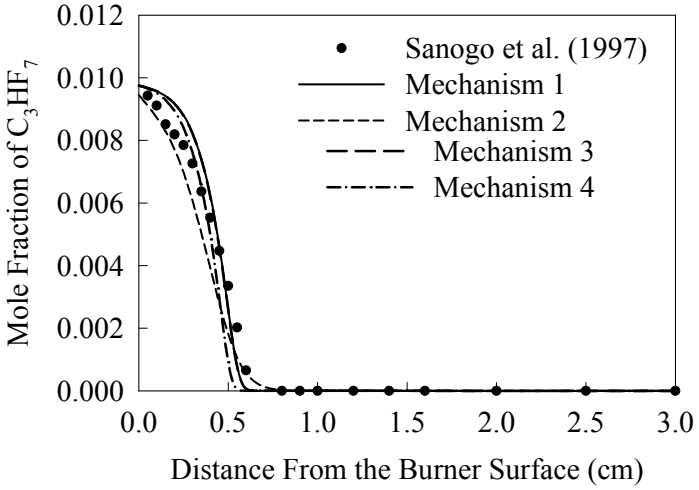

Figure 9: Comparison of the profiles of C_3HF_7 mole fraction produced by the mechanisms considered in this chapter with the experimental measurements of Sanogo et al. (1997); $CH_4/Ar/O_2/C_3HF_7 = 0.168/0.336/0.486/0.01$, $p = 0.042$ atm.

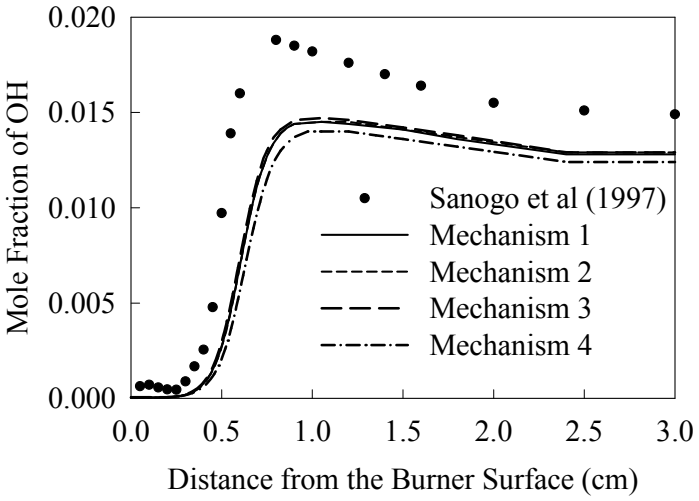

Figure 10: Comparison of the profiles of OH mole fraction produced by the mechanisms considered in this chapter with the experimental measurements of Sanogo et al. (1997); $CH_4/Ar/O_2/C_3HF_7 = 0.168/0.336/0.486/0.01$, $p = 0.042$ atm.

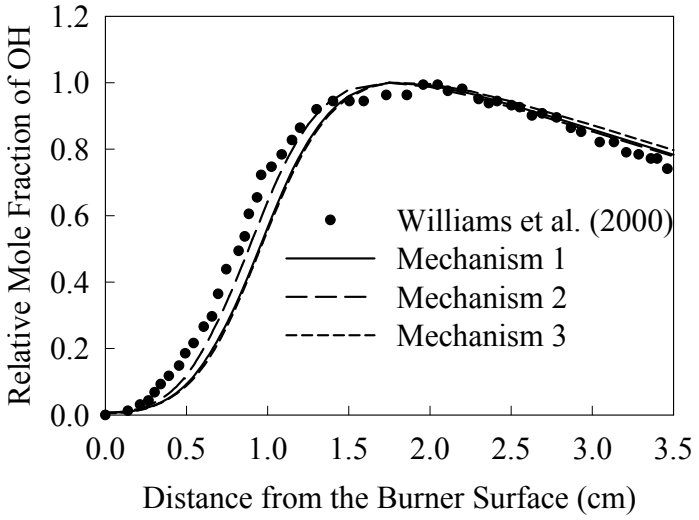

Figure 11: Comparison of the profiles of OH mole fraction obtained from LIF experiments (Williams et al., 2000) and from the models considered in this study; 4% C_3HF_7 and $p = 0.013$ atm.

Williams et al. (2000) employed laser-induced fluorescence (LIF) to measure the concentration of intermediate species H, OH, CH, CF, CF_2, and CHF for low pressure flames mitigated with C_3HF_7. Their results show a better agreement between the modelled and experimental results for the profile of OH radical. At least two factors can account for a better accuracy of LIF than MBMS measurements: (1) LIF is a non-intrusive technique and (2) LIF provides more accurate temperature measurements using LIF spectra of OH. LIF's temperature statistical uncertainty ranges from 20 – 45 K, while the temperature determined with thermocouples varies, between the low and high measurements, with uncertainty of 300

K, due to both the intrusive property of MBMS and accuracy of thermocouples. Note that, to calculate the results presented in Figure 11, we made the use of the temperature profile measured by Williams et al. (2000) and reported in Figure 1 of their paper.

CONCLUSIONS

Based on the analyses of the burning velocity, two modified inhibition mechanisms for flames doped with C_3HF_7 have been proposed, corresponding to the two existing mechanisms of Sanogo and Williams. The modified inhibition mechanisms improve the agreement between the predicted and measured burning velocity. For the comparison of the modelled flame structure for the major species with laboratory measurements, all inhibition mechanisms (including original inhibition mechanisms developed by Hynes et al., Sanogo et al. and Williams et al.) were examined against the same flame conditions, leading us to conclude that all mechanisms yield similar predictions of the flame structure. This means that the shorter, but less comprehensive, mechanism of Sanogo et al. offers an advantage of more rapid calculations, when one seeks only the concentration profiles of the major species. Finally, the imposition of the boundary condition of known mass fractions at the cold inlet of a premixed burner can improve the predictions of the concentration profiles of some major species profiles in low-pressure premixed flames.

REFERENCES

Biordi J. C., Lazzara C. P. and J. F. Papp (1976) *Combust. Flame* 26, 57-76.

Burgess Jr. D. R., Zachariah M. R., Tsang W. and P. R. Westmoreland (1995) *Prog. Energy and Comb. Sci.* 21, 453-529.

Cvetanovic R. J. (1987) *Journal of Physical and Chemical Reference Data* 16, 261-326.

Dlugogorski B. Z., Hichens R. K., Kennedy E. M. and J. W. Bozzelli (1998) *Proc. Saf. Env. Prot.* 76, 81-89.

Hamins A. and T. G. Cleary (1995) *International CFC and Halon Alternatives Conference & Exhibition - Stratospheric ozone Protection for the 90's*, Washington, DC, 664-673.

Harrison G. C. (1995) *ACS Symposium Series* 611 74-84.

Hranisavljevic J., Carroll J. J., Su M. C. and J. V. Michael (1998) *Int. J. Chem. Kin.* 30, 859-867.

Hynes R. G., Mackie J. C. and A. R. Masri (1998) *Combust. Flame* 113, 554-565.

Kee R. J., Rumpley F. M. and J. A. Miller (1989) *Chemkin-II: A Fortran Chemical Kinetics Package for the Analysis of Gas Phase Chemical Kinetics*, Report No.:Gov. Pub. SAND89-9009B.

Knyazev V. D., Bencsura A. and I. R. Slagle (1997) *J. of Phys. Chem. A* 101, 849-852.

L'Esperance D., Williams B. A. and J. W. Fleming (1999) *Combust. Flame* 117, 709-731.

Linteris G. T., Burgess Jr. D. R., Babushok V., Zachariah M., Tsang W. and P. Westmoreland (1998) *Combust. Flame* 113, 164-180.

Linteris G. T., Rumminger M. D. and V. I. Babushok (2000) *Combust. Flame* 122, 58-75.

Linteris G. T. and L. Truett (1996) *Combust. Flame* 105, 15-27.

Mackie J. C. (2003) *Thermophysical Parameters of Hydrofluorocarbon Species*, Private Communication.

Richter H., Vandooren J. and P. J. V. Tiggelen (1994) *Proc. Combust. Inst.* 25, 825-31.

Saito K., Kuroda H., Kakumoto T., Munechika H. and I. Murakami (1985) *Chem. Phys. Lett.* 113, 399-402.

Sanogo O., Delfau J. L., Akrich R. and C. Vovelle (1997) *Combust. Sci. Technol.* 122, 33-62.

Takahashi K., Inomata T., Abe T., Fukaya H., Hayashi E. and T. Ono (1998) *Combust. Sci. Technol.* 131, 187-191.

Tsai C. P. and D. L. McFadden (1989) *J. Phys. Chem.* 93, 2471-4.

Vovelle C. (2003) *Experimental Measurements of Premixed Methane Flames Mitigated with C_3HF_7*, Private Communication.

Williams B. A, L'Esperance D. M. and J. W. Fleming (2000) *Combust. Flame* 120, 160-172.

Yamamori Y., Takahashi K. and T. Inomata (1999) *J. Phys. Chem. A* 103, 8803-8811.

Zachariah M. R. and W. Tsang (1995) *J. Phys. Chem.* 99, 5308-18.